

## INTERPHASE SPACING IN DIRECTIONAL SOLIDIFICATION OF WHITE CARBIDE EUTECTIC

TREPCZYŃSKA-ŁENT Małgorzata

*UTP University of Science and Technology, Bydgoszcz, Poland, EU*

[malgorzata.trepczynska-lent@utp.edu.pl](mailto:malgorzata.trepczynska-lent@utp.edu.pl)

### Abstract

Directionally solidified sample of Fe-C alloy in a vacuum Bridgman-type furnace was produced under an argon atmosphere. The pulling rate was  $v = 83.3, 125.0$  and  $166.7 \mu\text{m/s}$  (300, 450 and 600 mm/h) with constant temperature gradient  $G = 33.5 \text{ K/mm}$ . The microstructure of the sample was examined on the longitudinal section using an optical microscope and scanning electron microscope. The average interphase spacing  $\lambda$  was measured on longitudinal section of the sample. The relationship between  $\lambda$  and  $v$  was determined using linear regression analysis.

**Keywords:** Directional solidification, white carbide eutectic, microstructure, interphase spacing

### 1. INTRODUCTION

Many engineering materials are based on eutectic alloys. This was the reason for extensive, both experimental and theoretical study of the relationship between solidification conditions and microstructure. An eutectic reaction may be defined as the instance where two (or more) distinctively different solid phases solidify simultaneously from the parent liquid [1-3].

The eutectic was studied for many years. The growth conditions governing formation of the various morphologies are still neither fully defined nor properly understood. Eutectics based on Fe-C make up the main of cast alloys. The unique combination of desirable properties and good castability is main reason for them to be widely used. The close control of the microstructure during solidification is necessary for such alloy's mechanical and physical properties optimization [4, 5]. An important stage during the solidification of white cast iron is eutectic solidification. The carbide in eutectic cells or eutectic carbide is the main hard and brittle structure which has an important effect on the properties of white cast iron [6-10].

Directional solidification technique is applied to the research on the basic solidification theory. Furthermore, it is used in manufacturing of high-performance products. Regular structures of fibrous or lamellar type may be obtained by directional solidification of binary or pseudo-binary eutectics. The parameters of unidirectional eutectics and their dependencies were widely studied [2, 3, 11-18].

The Jackson-Hunt model of the eutectic structures [19] is one of the most significant theoretical studies. This model provides relationship between the undercooling  $\Delta T$ , the growth rate  $v$  and the lamellar spacing  $\lambda$  for an isothermal solidification front as:

$$\Delta T = K_1 v \lambda + \frac{K_2}{\lambda} \quad (1)$$

$$\lambda_E^2 v = \frac{K_2}{K_1} = \text{constant} \quad (2)$$

where  $\lambda$  is the interphase spacing,  $v$  is the growth rate,  $K_1$  and  $K_2$  are system parameters [1].

**Figure 1** show schematic diagram of regular eutectic structure which forms under steady-state directional solidification conditions for  $\alpha$  and  $\beta$  phase [5, 12, 19].

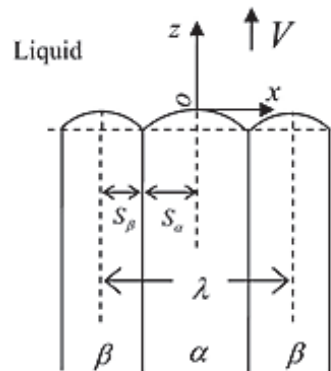


**Figure 1** Schematic diagram of the regular eutectic structure which defines the coordinate system [5]

## 2. EXPERIMENTAL PROCEDURES

The samples of eutectic were prepared in corundum crucible under the protection of argon gas in Balzers-type heater from pure Armco iron and pressed graphite with spectral purity 99.99 % C. The molten alloy was poured into permanent mold and cast into rod 12 mm in diameter after homogenization and impurities removal. Afterwards, using a wire cutting process, because of the high brittleness of the metals at this composition, these samples were machined to approximately 5 mm in diameter. **Table 1** presents the chemical composition of this alloy.

**Table 1** Chemical composition of Fe-C alloy

C	Si	Mn	P	S	Cr	Ni	Mo	Al	Cu	Co
4.25	0.057	0.64	0.0079	0.021	0.033	0.0093	<0.0020	0.011	0.032	0.0024
Ti	Ni	Nb	V	W	Pb	Mg	B	Sn	Zn	As
<0.0010	0.0093	<0.0040	0.0022	<0.010	<0.0030	<0.0010	0.0009	0.0061	<0.0020	0.0069
Bi	Ca	Ce	Zr	La	Fe					
<0.0020	0.0005	<0.0030	0.0043	0.0013	94.9					

The sample was positioned at the center of the vacuum Bridgman-type furnace in an alundum tube with inner diameter of 6 mm. Then it was heated to a temperature of 1450°C under an argon atmosphere. The sample was lowered at a given rate from the heating part to the cooling part of the furnace, with liquid alloy Ga-In-Sn used as the coolant after stabilizing the thermal conditions. The pulling process was performed at a selected growth rates of 83.3  $\mu\text{m/s}$ , 125.0  $\mu\text{m/s}$  and 166.7  $\mu\text{m/s}$ . The Pt40Rh-Pt20Rh thermocouple was used to measure the temperature gradient. In the experiments the  $G=33.5$  K/mm was constant. This procedure was described in more detail in [20].

The directional solidification was performed in the Faculty of Foundry Engineering at the AGH University of Science and Technology in Cracow.

## 3. MICROSTRUCTURE RESEARCH

Researched samples were on their longitudinal sections mechanically grinded, polished and etched using nital solution. The microstructure was examined on the longitudinal section using an optical microscope and scanning electron microscope. **Figure 2** show the polished and etched sample with marked growth direction.



**Figure 2** Image of the researched sample

#### 4. MEASUREMENT OF INTHERPHASE SPACING

The geometrical parameter  $\lambda$  measurements were made on the samples where the eutectic was oriented. The literature concerning volume metallography suggests [21] various methods of interphase spacing measurement in eutectic. In this case, the average interphase spacing in oriented eutectic was determined as a quotient of measure lines  $\sum L$  (perpendicular to the section) to the number of intersections  $f$  of these lines into white iron carbide precipitation:

$$\lambda = \frac{\sum L}{f} \tag{3}$$

Geometric parameter was also measured with picture analysis application - NIS-Elements. On the line, which was drawn perpendicularly to the axis and the longitudinal section, the distances between white iron carbide precipitations were measured, as the **Figure 3** presents. Then, the Microsoft Excel was used to calculate the parameters. Approximately 240 lines were measured in at least 4 different distances from the face of the sample and in 5 successive longitudinal sections of each sample. The obtained values were statistically verified.

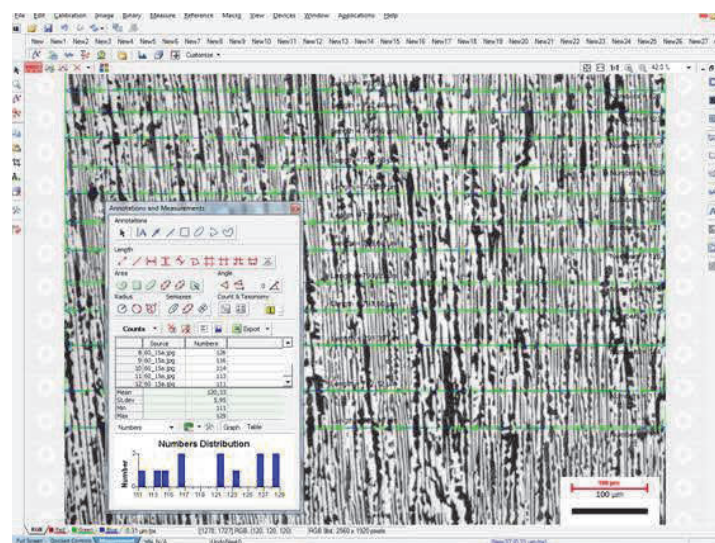


**Figure 3** Measurement method of the number of intersections  $f$  of these lines into iron carbide extraction

## 5. RESULTS

The **Figure 4** shows the microstructure of eutectic in the areas of obtained directional eutectic. On the **Figure 5** SEM eutectic microstructure are represented.

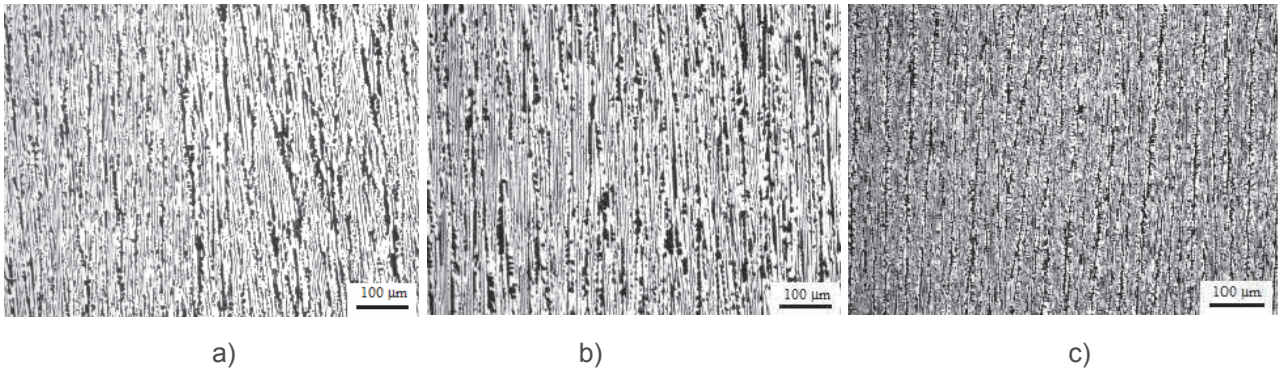


**Figure 4** Microstructure of Fe-C eutectic on the longitudinal section,  $G= 33.5$  K/mm a)  $v=83.3$   $\mu\text{m/s}$ , b)  $v=125.0$   $\mu\text{m/s}$ , c)  $v=166.7$   $\mu\text{m/s}$

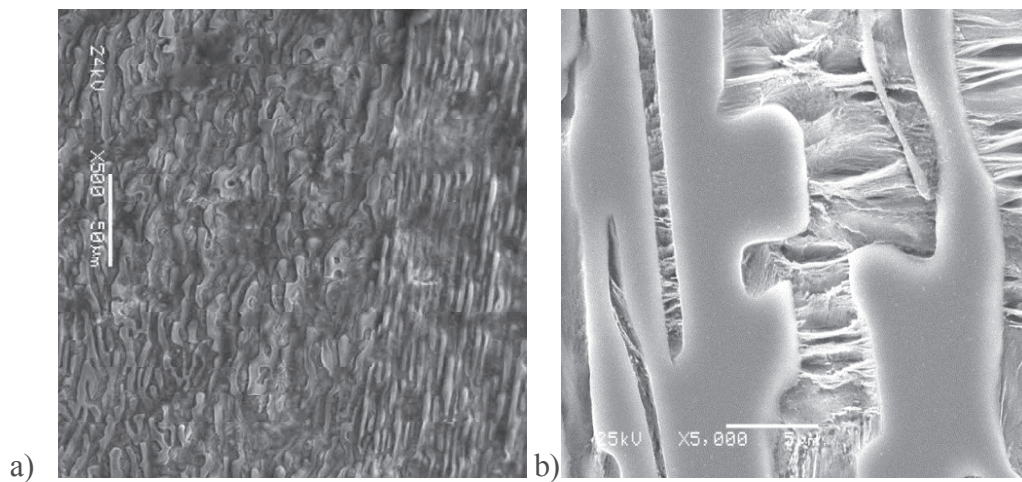


**Figure 5** Microstructure of Fe-C eutectic:  $v=83.3$   $\mu\text{m/s}$ ,  $G= 33.5$  K/mm, SEM; a) fracture of sample; b) on the longitudinal section

The growth conditions and measurements for Fe-C eutectic are given in **Table 2**. The dependence of average interphase spacing on growth rates as a function of the inverse square root of the growth rate is shown in **Figure 6**.

**Table 2** Growth conditions and measurements for Fe-C eutectic

Condition	$G$ K/mm	$v$ $\mu\text{m/s}$ (mm/h)	$\lambda$ $\mu\text{m}$	$v^{-0,5}$ $\sqrt{s/\mu\text{m}}$
1	33.5	83.3 (300)	$8.25 \pm 0,58$	0.109566
2		125.0 (450)	$6.18 \pm 0,39$	0.089443
3		166.7 (600)	$4.87 \pm 0,37$	0.077452

## 6. DISCUSSION

As can be seen from **Figure 4** during eutectic growth, a large number of eutectic grains can be formed. All grains seem to be oriented parallel to growth direction. This structure is clearly vertically directed. It was created during directional solidification using the Bridgman method.

In a longitudinal section, the interphase spacing seems to be different in each grain. This was caused by different cutting angles to the polished surface. That is the reason why the average spacing was made.

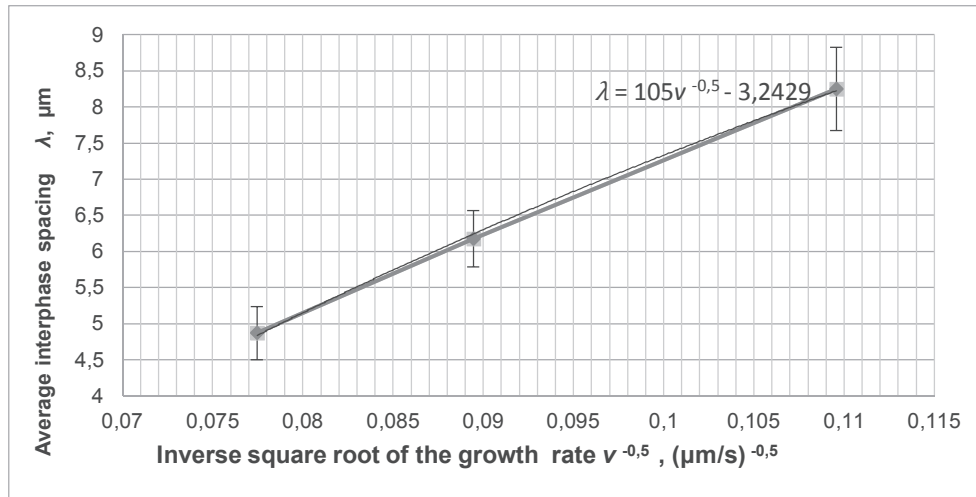


**Figure 6** Average interphase spacing as a function of the inverse square root of the growth rate,  $G=33.5$  K/mm

With a change of pulling rate, differences in the size of formed eutectic can be seen. **Figure 4** show the microstructures become finer with increasing growth rate. During the solidification process, the dimensions of created microstructure are dependent on the atomic diffusion ability. The increase of growth rate leads to high temperature gradient at the front of solid-liquid interface. Increase of cooling rate causes the decrease of atomic diffusion ability. This means that the available diffusion distance is shortened. So, the higher growth rate, the finer the resultant microstructure.

The eutectic mixture is represented by the vertically elongated white lamellar structure and dark regions. The white regions have been identified as  $\text{Fe}_3\text{C}$  iron carbide [22].

On **Figure 5a** the fracture morphology of sample is shown. Parallel to each other lamellar structures of  $\text{Fe}_3\text{C}$  iron carbide can be seen.

As the SEM images in **Figure 5b** show, between these white lamellar structures there are fine flakes. EBSD measurements [22] identified these regions as alpha iron (ferrite). Because these samples were etched in nital - the iron phase is dark after etching process as it has transformed to a fine pearlite structure. This is consistent with the SEM micrograph on **Figure 5b**. The longitudinal section on **Figure 4** illustrates that many of these dark regions have a rod fibers morphology.

The shapes of the curves, of the relationship between average interphase spacing  $\lambda$  as a function of the inverse square root of the growth rate on **Figure 6**, are characteristic for eutectic structures [1,2,6,7]. Therefore examined white carbide alloy is an eutectic. Previous measurements done with the XRD and EBSD techniques [22] also have shown that the obtained alloy is a white carbide eutectic.

In [7] a comparison of the published results for the white eutectic  $\text{Fe}-\text{Fe}_3\text{C}$  was made and the appropriate calculations were made to obtain the relation  $\lambda = 20.1v^{-0.5}$ . Research results [7] of pure  $\text{Fe}-4.3$  wt pct C alloys led to the equation  $\lambda = 0.821 + 12.2v^{-0.5}$ . The temperature gradients  $G$  in these studies had different values.

## 7. CONCLUSION

As a result of directional solidification of Fe-4.25 wt pct C alloy, with pulling growth 83.3  $\mu\text{m/s}$ , 125.0  $\mu\text{m/s}$  and 166.7  $\mu\text{m/s}$ , unidirectional white carbide eutectic were obtained.

The relationship between average interphase spacing  $\lambda$  and growth rate  $v$  (in the growth rate range of 83.3 to 166.7  $\mu\text{m/s}$ ) at constant temperature gradient  $G=33.5$  K/mm was determined:  $\lambda = 105v^{-0.5} - 3.2429$ . This result may be related to the faceted nature of the  $\text{Fe}_3\text{C}$  component of the white carbide eutectic. This equation differs from those presented in [7]. The reason may be different  $G$  temperature gradients. The data of the interphase spacing (**Figure 6**) do not fit the standard theoretical model of  $\lambda^2v = \text{constant}$ .

## ACKNOWLEDGEMENTS

**The author wishes to express gratitude to Prof. E. Guzik, PhD E. Olejnik and PhD A. Janas from Faculty of Foundry Engineering, Department of Engineering of Cast Alloys and Composites at AGH in Cracow.**

## REFERENCES

- [1] MAGNIN, P., KURZ, W. An analytical model of irregular eutectic growth and its application to Fe-C. *Acta Metallurgica*, 1987, vol. 5, no. 35, pp. 1119-1128.
- [2] KAYA, H., ÇADIRLI, E., GUNDUZ, M. Eutectic growth of unidirectionally solidified bismuth-cadmium alloy. *Journal of Materials Processing Technology*, 2007, vol. 1101, no.183, pp. 310-320.
- [3] GUNDUZ, M., KAYA, H., ÇADIRLI, E., OZME, A. Interflake spacings and undercoolings in Al-Si irregular eutectic alloy. *Material Science and Engineering A*, 2004, vol. 3690, pp. 215-229.
- [4] JONES, H., KURZ, W. Growth temperatures and the limits of coupled growth in unidirectional solidification of Fe-C alloys. *Metallurgical Transactions*, 1980, vol. 11A, pp. 1265-1273.
- [5] MAGNIN, P., TRIVRDI, R. Eutectic growth: a modification of the Jackson and Hunt theory. *Acta Metallurgica et Materialia*, 1991, vol. 39, pp. 453-467.
- [6] JONES, H., KURZ, W., Relation of interphase spacing and growth velocity in Fe-C and Fe- $\text{Fe}_3\text{C}$  eutectic alloys. *Zeitschrift für Metallkunde*, 1981, vol. 91, p. 792.
- [7] PARK, J.S., VERHOEVEN, J.D. Directional solidification of white cast iron. *Metallurgical and Materials Transactions A*, 1996, vol. 27A, pp. 2328-2337.
- [8] JIYANG Z. Chapter 5 - White cast iron. In *Colour metallography of cast iron*. China Foundry, 2009, 447- 462 p.
- [9] NASTAC, L., STEFANESCU, D.M. Prediction of gray to white transition in cast iron by solidification modeling, *AFS Transactions* 1995, vol. 10, pp. 329-337.
- [10] HILLERT, M., SODERHOLM, P. White and grey solidification of the Fe-C-P eutectic. The Metallurgy of cast iron. *Georgi Publishing Company Geneva, Switzerland*, 1974, pp. 197-206.
- [11] ÇADIRLI, E., GUNDUZ, M. The dependence of lamellar spacing on growth rate and temperature gradient in the lead-tin eutectic alloy. *Journal of Materials Processing Technology*, 200, vol. 97, pp. 74-81.
- [12] LIU, L., LI, J., ZHOU, Y. Solidification of undercooled eutectic alloys containing a third element. *Acta Materialia*, 2009, vol. 57, pp. 1536-1545.
- [13] VERHOEVEN, J.D., PARK, J.S., JONES, L. Effect of Te on morphological transitions in Fe-C-Si alloys. Part 1 Directional solidification. *Metallurgical and Materials Transactions A*, 1989, vol. 20A, no. 9, pp. 1867-1873.
- [14] WOŁCZYŃSKI, W. Role of physical factors in solid - liquid interface formation during oriented eutectic growth, *Crystal Research and Technology*, 1990, vol. 14, no. 1, pp. 1303-1309.
- [15] WOŁCZYŃSKI, W. Contribution to transition layer determination for oriented eutectic growth. *Crystal Research and Technology*, 1990, vol. 25, no. 12, pp. 1433-1437.
- [16] WOŁCZYŃSKI, W. Formation of concave-convex interface shape during oriented eutectic growth. *Crystal Research and Technology*, 1991, vol. 26, no. 2, pp. 173-178.

- [17] GUZIK, E. A model of irregular eutectic growth taking as an example the graphite eutectic in Fe-C alloys. *Dissertations Monographies 15, AGH Cracow*, 1994.
- [18] GUZIK, E., KOPYCIŃSKI, D. Modelling structure parameters of irregular eutectic growth: Modification of Magnin-Kurz theory. *Metallurgical and Materials Transactions A*, 2006, vol. 37A, pp. 3057-3067.
- [19] JACKSON, K.A., HUNT, J.D. Lamellar and rod eutectic growth. *Transactions of the Metallurgy Society of AIME*, 1966, vol. 236, pp. 1129-1142.
- [20] TREPCZYŃSKA-ŁENT, M. Possibilities of the materials properties improvement for the cementite eutectic by means of unidirectional solidification. *Archives of Metallurgy and Materials*, 2013, vol. 58, no.3, pp. 987-991.
- [21] RYŚ, J. Quantitative metallography, *AGH Cracow*, 1983.
- [22] TREPCZYŃSKA-ŁENT, M. XRD and EBSD measurements of directional solidification Fe-C eutectic alloy. *Archives of Foundry Engineering*, 2016, vol. 16, no. 4, pp. 169-174.